REGULAR PAPER

Brazing in SiH₄-Doped Inert Gases: A New Approach to an Environment Friendly Production Process

Ulrich Holländer[1] · Daniel Wulff[1] · André Langohr[1] · Kai Möhwald[1] · Hans Jürgen Maier[1]

Abstract

Engineering under protective atmospheres or in vacuum allows the production of materials and components, where the absence of oxygen is an essential requirement for a successful processing. Ideally, joining or coating of (and with) metallic materials needs oxide free material surfaces, in order to achieve durable joints or coatings. Using the established technology of brazing in controlled atmosphere, fundamental physical mechanisms for deoxidation of metal surfaces are presented and the role of oxygen and water residue in the process atmosphere is analyzed. Furthermore, the doping of gases with monosilane for generating virtually oxygen-free process atmospheres is introduced and its advantages for an oxygen-free production are discussed.

Keywords Brazing · Inert gas · Monosilane · Deoxidation · Physical model · Production

Abbreviations

M_xO_{2y}	Metal oxide (stoichiometric indices x and 2y)
$\Delta_f G^0$	Standard free enthalpy of formation referred to 2 mol O
R	Gas constant (8.3144 mol J^{-1} K^{-1})
a_i	Activity of component i
M_i	Molar mass of component i
ρ_i	Density of component i
D_O	Diffusion coefficient of oxygen
X_i	Substance concentration of component i
w_i	Mass fraction of component i
K_a	Equilibrium constant referred to activities of reactants
^1N_O	Number of oxygen atoms per unit volume
N_A	Avogadro constant (6.022 × 10^{23} mol^{-1})
J_O	Mass flow of oxygen
d	Thickness of oxide layer

1 Introduction

The vast majority of processes in the metal-working is performed in the presence of oxygen and humidity. As a result, a rapid oxidation of the metal surfaces takes place. The actual thickness of the oxide layer formed depends on the process temperature and the reactivity of the metal. While passivating oxide layers usually have a positive effect on the performance of the finished work pieces due to the resulting corrosion protection, they are a disruptive factor in numerous important production processes like welding, brazing or coating in all their facets. Therefore, extensive efforts are necessary to remove the oxide layers directly before or during these processes. Depending on the actual process, this is typically performed by a mechanical (grinding, grit blasting etc.) and/or chemical treatment (acid cleaning, use of flux etc.). In terms of both environmental impact and work safety both approaches are critical. Especially the use of chemicals for such cleaning procedures is increasingly restricted by stringent rules and regulations.

In demanding (elevated temperature) processes, the oxygen (and humidity) concentration in the surrounding process atmosphere is drastically reduced by the use of inert gases or by transferring the process into a vacuum chamber. The heat treatment of workpieces in furnaces (conveyor belt furnace, vacuum furnace), e.g. for brazing or sintering, is a well-known example. However, the conditions in these processes are in fact not "oxygen-free". Conventional protective gases used for typical processes have oxygen (and water) residues of about 5 ppm and even in an excellent high vacuum furnace with a residual pressure of 10^{-6} mbar, component surfaces are still bombarded by oxygen molecules in the order of well over 10^{12} wall collisions per square centimeter each second.

✉ Ulrich Holländer
hollaender@iw.uni-hannover.de

[1] Institut für Werkstoffkunde (Materials Science), Leibniz Universität Hannover, 30823 Garbsen, Germany

🙋 Springer KSPE

In order to understand the consequences of the contamination with oxygen or water vapour for the different processes, a careful analysis of the physicochemical reactions between the metallic surfaces and the protective atmospheres containing small amounts of oxygen is paramount. In this context, flux-free brazing processes in controlled atmosphere provide for a good reference. This type of "oxygen-free" production is well established and a multitude of structural materials have been joined successfully by brazing in furnaces.

Initially, the material features a native oxide layer, and thus, deoxidation is a key step in a brazing process. Various theories have been proposed in literature to explain the removal of oxide layers from the surface during brazing in absence of reducing atmosphere or a flux [1]. Especially for high-vacuum brazing processes it has been assumed, that thermal decomposition of oxide layers may take place or the oxide simply evaporates without prior decomposing. Another explanation is, that the mismatch of thermal expansion between the oxide and its metallic substrate leads to cracks in the oxide layer upon heating. Subsequently, the cracks are infiltrated by molten filler metal, which is assumed to lead to a delamination of the oxide layer. Furthermore, in the case of steel alloys it may be possible, that carbon as an inevitable residue even in stainless steel may serve as an internal reducing agent for the oxide (releasing carbon monoxide then), a theory which is at least thermodynamically reasonable [2]. However, none of these theories have been verified (or falsified) experimentally so far, as measuring the various nano-scaled physical or chemical effects stated is extremely difficult especially under brazing process conditions.

In the following, a physical model is introduced, describing a diffusion controlled mechanism of surface deoxidation when brazing stainless steel. Based on the analysis, requirements and limits for successful brazing processes are derived. Furthermore, the use of monosilane-doped inert gases as an alternative to conventional hydrogen as a process gas with extremely low oxygen activity is presented. It is shown, that the idea of an oxygen-free environment can be realised almost perfectly using small amounts of monosilane as an additive to the process gas. Finally, the advantages of using monosilane-doped process gases instead of hydrogen are discussed with view on an environmental friendly production.

2 Mechanism of Steel Deoxidation During High Temperature Brazing in Inert Process Atmospheres

Flux-free brazing of steel components under shielding gas or in high vacuum furnaces are widely used industrial examples, where the absence of oxygen is essential for successful
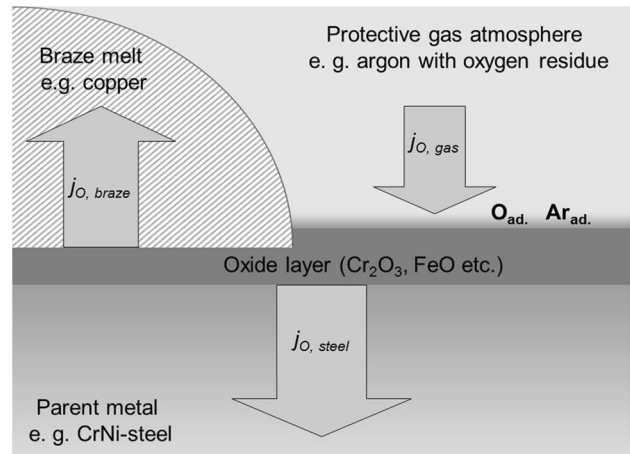

Fig. 1 Oxygen mass flows in a flux free brazing process under protective gas

joining. Prerequisites are carefully controlled process atmospheres and elevated brazing temperatures, in order to initiate physico-chemical processes, which yield oxide-free metal surfaces suitable to be wetted with the braze metal [3]. Especially in absence of an oxide reducing agent like hydrogen the level of oxygen and water residue in the process gas has to be extremely low, in order to avoid re-oxidation of the surfaces. In this case the degradation of oxide layers is possible only by thermally activated diffusion processes, which are mainly governed by the type of material (parent metal and braze alloy) and the temperature–time-regime of the brazing process. Figure 1 illustrates the oxygen mass flows, which occur during brazing and—if balanced in the right way—can lead to the degradation of native oxide layers in inert gases with minimal oxygen residue. In the case of a vacuum furnace the oxygen content (equivalent to the partial oxygen pressure) affecting the materials' surfaces is governed by the vacuum level (typically 10^{-5} mbar to 10^{-4} mbar) in the vacuum chamber.

In the present paper, two different scenarios are considered in order to simulate the conditions for oxide layer decomposition during brazing: (1) the oxidised surface is already covered with braze metal and no contact to the process atmosphere takes place. (2) the oxidised surface is exposed in the process atmosphere and a further oxygen uptake by chemisorption of gaseous oxygen (or water vapor) is possible.

(i) Oxide layer covered with braze metal

In this case three thermodynamic subsystems exist, i.e. the parent metal, its oxide layer and the contacting (liquid) braze metal. Through the common system boundaries (interfaces) an exchange of heat and material is possible, such that the whole system is able to reach thermodynamic equilibrium in principle. The subsystems seek to equal different chemical

potentials and thermodynamic activities, respectively, of each chemical component by interdiffusion. In the current context, the diffusion of oxygen from the oxide layer into the metallic substrate is of special interest, and it is assumed that this is the rate controlling step of the oxide layer degradation.

In order to analyze the oxygen diffusion, it is necessary to know the resulting concentration of oxygen in the metal at the phase boundary to the oxide. The thermodynamic activity of oxygen in a metal oxide layer can evaluated using the reaction:

$$\frac{x}{y}M + 2O \leftrightarrow \frac{1}{y}M_xO_{2y}. \tag{1}$$

The equilibrium constant of this reaction with respect to the activities is given by

$$K_a(T) = \frac{\left[a_{M_xO_{2y}}\right]^{\frac{1}{y}}}{\left[a_M\right]^{\frac{x}{y}}[a_O]^2}. \tag{2}$$

By definition, activities of pure condensed phases in a reaction system are equal to 1, i.e.

$$a_{M_xO_{2y}} = a_M = 1. \tag{3}$$

The equilibrium constant in Eq. (2) is correlated with the standard free enthalpy $\Delta_f G(T)^0$ of the oxide formation (Eq. 1) by

$$\Delta_f G^0_{M_xO_{2y}}(T) = -RT \ln K_a(T). \tag{4}$$

From this the oxygen activity in a metal oxide is obtained as:

$$a_O = \exp\left(\frac{\Delta_f G^O_{M_xO_{2y}}(T)}{2RT}\right). \tag{5}$$

Assuming thermodynamic equilibrium at the phase boundary this measure is identical to the oxygen activity in the contacting metals (braze melts and parent metal, respectively) at the interfaces. The activity a_i and concentration X_i of a component i in a given mixture is:

$$a_i = X_i \times \gamma_i(T, X_i). \tag{6}$$

Here, the activity coefficient γ_i is again a mixture-specific function of temperature and concentration. Knowing the oxygen concentration at a given oxygen activity (Eq. 5) in the metal at the interface from Eq. (6), Fick's 2nd law can be applied to evaluate the oxygen diffusion rate from the oxide layer into the metal substrate:

$$N_{O,Diff}(x,t) = A \times {}^1N_O\left(1 - \mathrm{erf}\left[\frac{x}{2\sqrt{D_Ot}}\right]\right). \tag{7}$$

In Eq. (7) D_O is the oxygen diffusion coefficient in the metal and ${}^1N_O$ is number of oxygen atoms per volume at the phase boundary, calculated from

$${}^1N_O = X_O \times \frac{\rho_{metal}}{M_{metal}}N_A, \tag{8}$$

using the density as well as the molar mass of the metal and the Avogadro constant N_A (6022×10^{23} mol^{-1}).

Differentiating Eq. (7) with respect to x at $x = 0$ gives the actual concentration gradient of oxygen at the interface. Multiplying this with the diffusion coefficient D_O results—according to Fick's 1st law—in the corresponding oxygen mass flow per unit area A from the oxide layer into the metal substrate:

$$J_{O,diffusion}(t) = \frac{1}{A}\frac{dN}{dt} = -{}^1N_O\sqrt{\frac{D_O}{\pi t}}. \tag{9}$$

Finally, integration of Eq. (9) with respect to the time t yields the amount of oxygen per unit area diffused from the oxide layer into the metal:

$$\frac{\Delta N_{O,diffusion}(t)}{A} = \int_0^t J_{O,diffusion}(t)dt = -2\,{}^1N_O\sqrt{\frac{D_Ot}{\pi}}. \tag{10}$$

The amount of oxygen transported is related to the oxide layer degradation rate, Δd, via its chemical stoichiometry (M_xO_{2y}), molar mass $M_{M_xO_{2y}}$ and density $\rho_{M_xO_{2y}}$:

$$\Delta d(t) = \frac{\Delta N_{O,diffusion}(t)}{A}\frac{M_{M_xO_{2y}}}{2y\rho_{M_xO_{2y}}N_A}. \tag{11}$$

The physical relations used above are applicable provided that the necessary thermodynamic and kinetic data (free enthalpies of oxide formation, oxygen activities and diffusion coefficients) of the materials considered are available. In the case of steel and simple braze metals like pure copper or binary silver copper alloys the corresponding data can be extracted from literature.

Firstly, the oxygen activities of the relevant oxides for stainless steel are evaluated according to Eq. (5) using parameters from [4], listed in Table 1.

According to [5] the thermodynamic activity coefficient of oxygen in liquid copper is related to its concentration by the numerical equation:

$$\log \gamma_{O,Cu} = \left(\frac{-4300\,\mathrm{K}}{T/\mathrm{K}} + 2.399\right) + \left(\frac{-1350\,\mathrm{K}}{T/\mathrm{K}} + 5.59\right)X_{O,Cu}. \tag{12}$$

The necessary data for liquid silver are not available. Because of the chemical similarity to copper and similar binary phase diagrams (Cu–O and Ag–O) it is assumed therefore, that the concentration and temperature dependence

Table 1 Parameter for evaluating the free enthalpies of oxide formation

Reaction	$\Delta_f G^o_{M_x O_{2y}}(T) = \alpha + \beta T$	
	α/J	β/J/K
$Fe + O_2 = 2FeO$	$-518{,}986$	125.042
$6FeO + O_2 = 2Fe_3O_4$	$-624{,}122$	250.084
$4/3Cr + O_2 = 2/3Cr_2O_3$	$-746{,}487$	171.88

Table 2 Materials data of relevant metal oxides for oxide layer on steel corresponding to Eq. (11)

M_xO_{2y}	$M_{M_xO_{2y}}$ g/mol	$2y$	$\rho_{M_xO_{2y}}$ g/cm^3	$\frac{M_{M_xO_{2y}}}{2y\rho_{M_xO_{2y}}N_A}$ cm^3
Cr_2O_3	152	3	5.22	1.61×10^{-23}
FeO	71.9	1	6.0	2.00×10^{-23}
Fe_3O_4	231.5	4	5.2	1.85×10^{-23}

Densities of oxides from [10]

of oxygen activity in silver at low oxygen concentrations is similar to that of copper, so that Eq. (12) can be also used, for extrapolating the activity coefficients to temperatures lower than 1084 °C for liquid Ag–Cu alloys. For γ-Fe, numerous experimentally determined oxygen activities are available and the data can be described by Eq. (13) from Ref. [6]:

$$w_{O,\gamma-steel}/wt. - \% = 8.511 \times 10^{-4} \times 10^{\left(\frac{9030}{T/K}\right)} a_{O,\gamma-steel}. \quad (13)$$

Here the resulting oxygen mass concentration is related to its substance ratio by

$$X_{O,\gamma-steel} = \frac{1}{1 + \frac{1-w_{O,\gamma-steel}}{w_{O,\gamma-steel}}\frac{M_{Fe}}{M_O}}. \quad (14)$$

In addition the temperature dependent diffusion coefficients of oxygen in the various metals are needed for the physical modelling, see Eq. (10). For numerical evaluation the following Arrhenius relations were used for Cu and Ag [7] as well as γ-steel [8]:

$$D_{O,Cu} = 6.9 \times 10^{-7} m^2/s \times \exp\left(-\frac{53948\,J/mol}{RT}\right) \quad (15)$$

$$D_{O,Ag} = 2.8 \times 10^{-7} m^2/s \times \exp\left(-\frac{34711\,J/mol}{RT}\right) \quad (16)$$

$$D_{O,\gamma-steel} = 1.3 \times 10^{-4} m^2/s \times \exp\left(-\frac{166000\,J/mol}{RT}\right). \quad (17)$$

The oxygen diffusion coefficients in the eutectic AgCu brazing alloy (28 wt% Cu: $X_{Cu} = 0.401$) can be determined using the linear interpolation

$$D_{O,Ag72Cu28} = X_{Cu}D_{O,Cu} + (1 - X_{Cu})D_{Ag}. \quad (18)$$

Finally, the relation between the oxygen rate diffusing from the oxide layer into the bulk and the rate of layer degradation, given by Eq. (11), can be assessed using the data from Table 2.

Exemplary results of such calculations for brazing chromium containing austenitic steels with eutectic 72Ag-28Cu braze and pure Cu, respectively, are shown in Fig. 2. The
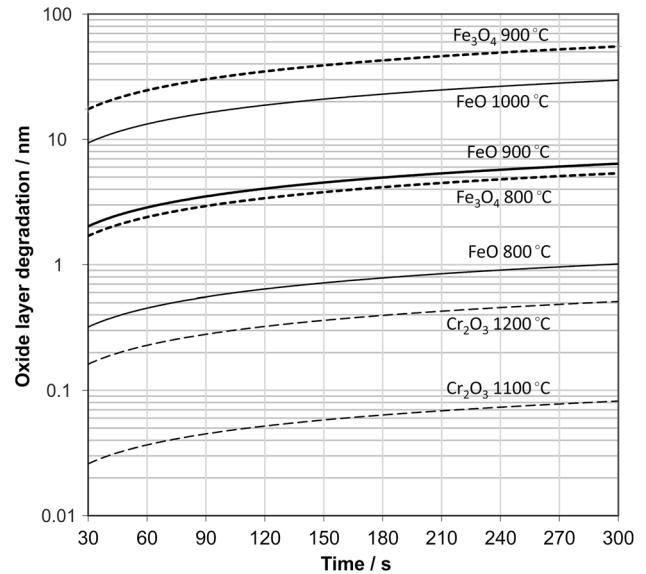

Fig. 2 Modelled oxide layer degradation rate as a function of dwell time at different temperatures; data shown are for different oxides and braze metals: Ag$_{72}$Cu$_{28}$ for 800–1000 °C and Cu for 1100 °C and 1200 °C

diagram displays the modelled oxide layer degradation rate with the time for various types of oxides (FeO, Fe$_3$O$_4$, Cr$_2$O$_3$) and brazing temperatures between 800 and 1200 °C. The model accounts for both, the oxygen diffusion into the liquid braze metal as well as into the solid steel. Here, oxygen diffusion into the braze metal amounts to typically 80% of the degradation of the oxide layer. The degradation rates do increase drastically with the decrease of the thermodynamic oxide stability in the sequence Cr$_2$O$_3$, FeO, Fe$_3$O$_4$. Native oxide layers on chromium steels are complex mixtures of all three oxides with a chromium oxide content of typically 30% and layer thickness of only 5 nm [9].

According to Fig. 2, a complete degradation of the iron oxides in such layers is expected already at 900 °C and 5 min dwell time, while the chromium oxide will remain essentially unchanged under this condition. Even at 1200 °C the degradation rate of chromium oxide is still very low (0.4 nm in 5 min), which implies that in typical brazing processes the elimination

of such a stable oxide does not happen completely without additional processes that assist deoxidation (e.g. oxide reducing agents like hydrogen in the process, see below). Actually for a successful brazing, it is unclear so far, to what extend a native oxide layer on stainless steel must be removed on an atomic scale, before a wetting with the braze takes place, see also discussion below.

(ii) Oxide layer exposed to the process atmosphere

In order to ensure a spreading of the braze metal over the substrate surface (e.g. to realise a capillary flow into a joining gap), the condition of the parent metal surface exposed to the process atmosphere has to be considered. With respect to the oxide layer, the diffusion of oxygen into the substrate as described above is still valid. In addition, transport of oxygen from the gas phase to the surface must now be taken into account as well. This results in an adsorbed oxygen layer on the surface, giving rise to further oxidation of the metal surface. The corresponding mass flow can be estimated using the kinetic theory of gases. The number of collisions per unit time and area, z_i, with a surface exposed to a gas is given by

$$z_i = \frac{p_i N_A}{\sqrt{2\pi M_i RT}}, \tag{19}$$

where M_i is the molar mass of the gas particle i, p_i is its pressure and R is the gas constant.

In the case discussed here a gas mixture has to be considered, which mainly consist of an inert gas (e.g. Ar) with the pressure p_{Ar} (approx. 100 kPa in an inert gas furnace) containing oxygen residues of $p_{O_2} < 10$ Pa (equal to 100 ppm residue). Few oxygen molecules compete therefore with many argon atoms for adsorption places on the surface. The probability for oxygen molecules finding a free place is given by the ratio r of oxygen particle collisions to all particle collisions with the surface:

$$r = \frac{z_{w,oxygen}}{z_{w,oxygen} + z_{w,argon}} \approx \frac{z_{w,oxygen}}{z_{w,argon}}. \tag{20}$$

Consequently, the mass flow of successfully adsorbed atomic oxygen on a metal surface is the product $2z_{oxygen}w$ as one O_2 molecule gives 2 O atoms, yielding

$$J_{O,gasphase} = \frac{2z_{oxygen}^2}{z_{Ar}}$$
$$= \frac{2p_{oxygen}^2 N_A}{p_{Ar}\sqrt{2\pi \frac{M_{O_2}^2}{M_{Ar}}RT}}. \tag{21}$$

Note that the number of adsorbed oxygen atoms per unit area and time is proportional to the square of the oxygen partial pressure. Again, the mass flow is a function of the temperature, but in contrast to the mass flow via diffusion into the bulk (Eq. 9) it is constant with respect to time. Thus, the amount of oxygen atoms per unit area transported to the surface after a certain time t is simply

$$\frac{\Delta N_O(t)_{absorbed}}{A} = J_{O,gasphase}t. \tag{22}$$

With respect to oxide layer degradation the sum of transported oxygen from the gas phase (Eq. 22) and the oxygen loss due to diffusion into the substrate (Eq. 10) is important:

$$\frac{\Delta N_{O,overall}(t)}{A} = J_{O,gasphase}t - 2^1 N_O \sqrt{\frac{D_O t}{\pi}}. \tag{23}$$

If this oxygen flow balance is negative a degradation of the oxide layer takes place. In the case of a positive value a further growth of the oxide layer can be expected.

In Figs. 3 and 4 computations of the oxygen flow balance according to Eq. (23) are summarised for FeO and Cr_2O_3 layers at temperatures from 800 to 1200 °C. In the calculation residual oxygen contents in the gas from 0.1 to 10 ppm were assumed. The value of 10 ppm corresponds to the typical value that can be realized in industrial furnace processes using inert gas. The lower contents (1 ppm in case of FeO and 0.1 ppm for Cr_2O_3) are hardly reached in industrial furnace processes due to the limited purity of industrial gases.

Note that for an appropriate scaling of the strongly differing curves two different y-axes where chosen in the diagrams in Figs. 3 and 4. For each curve, the arrows indicate the corresponding y-axis. According to Eq. (11) a negative (positive) oxygen flow balance of 10^{18} atoms/m² corresponds to a hypothetical oxide layer degradation (growth) of about 4 nm. The calculated curves for FeO indicate that the necessary conditions for a deoxidation of iron oxide layers are only achieved in process gases with 1 ppm oxygen residue, when the process temperatures are at least 1000 °C, whereas with 10 ppm always a further growth of oxide layer with a rate of roughly 1 nm/min is expected.

In the case of chromium oxide layer, even at high temperature (1200 °C) and very low oxygen residue (0.1 ppm) in the process gas no significant oxide degradation can be achieved, i.e. only -2.8×10^{-14} atoms/m² in 500 s, equivalent to a nominal thickness reduction of 0.01 nm. With 10 ppm O_2 residue a further growth of chromium oxide on the surface with similar rates as on iron takes place at temperatures between 800 and 1200 °C, which clearly leads to wetting problems when brazing.

Therefore, reducing the oxygen residue level to very low values prevents rather from a further formation of Cr_2O_3, than leads to a significant decomposition of already existing
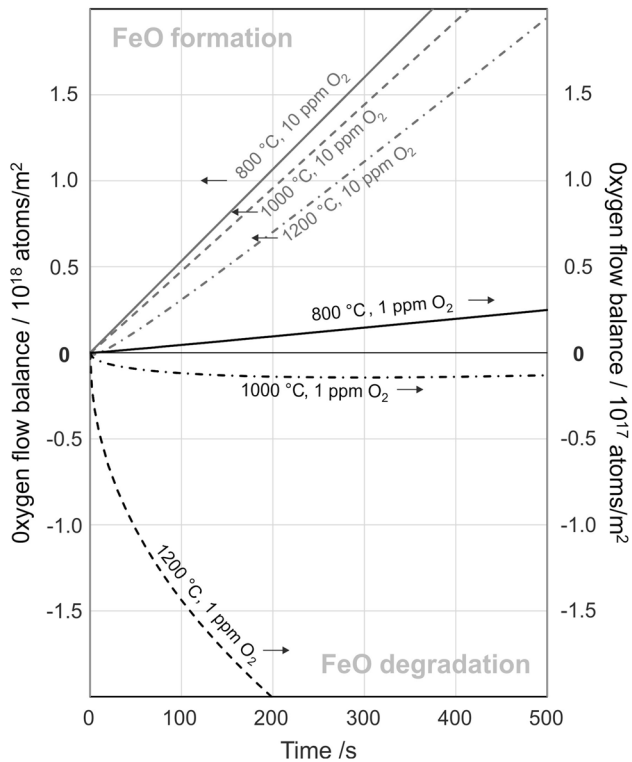
Fig. 3 Calculated oxygen flow balance curves for FeO as function of time for oxide layers on steel exposed to argon with two different residual oxygen contents (1 ppm, 10 ppm) at 800 °C, 1000 °C and 1200 °C; arrows indicate to which y-axis the curves are related to

Fig. 4 Calculated oxygen flow balance curves for Cr_2O_3 as function of time for oxide layers on steel exposed in argon with two different oxygen residues (0.1 ppm, 10 ppm) at 800 °C, 1000 °C and 1200 °C; arrows indicate to which y-axis the curves are related to

chromium oxide in the form of a native layer. Again, native oxide layers on stainless steel are nano-scaled mixtures of various iron oxides and Cr_2O_3, where at least the iron oxides could degrade by heat treatment according to the results presented. It is unclear what happens then with the remaining Cr_2O_3. In the case of discrete nano-crystallites, remaining on an otherwise deoxidated steel surface, a wetting with braze metal is certainly possible. While this is a total different mechanism of oxide layer degradation, the resulting effect would be similar to the idea of thermally initiated cracks in the oxide layer as a starting point for a penetration and oxide layer detachment by molten braze metal.

Although the presented physical approach, i.e. modelling oxide layer degradation based on thermodynamic stability and basic transport mechanism of oxygen in the different phases involved in the brazing process, is straightforward, the requirements and the limiting conditions for a successful wetting process are described quantitatively for the first time. The results obtained agree quite well with practical experiences from brazing steels in furnaces. For instance, the wettability of austenitic CrNi steel with AgCu brazes is sufficient for reliable capillary gap filling only at temperatures > 1000 °C and appropriate process atmospheres (under vacuum with < 10^{-4} mbar or under inert gas with
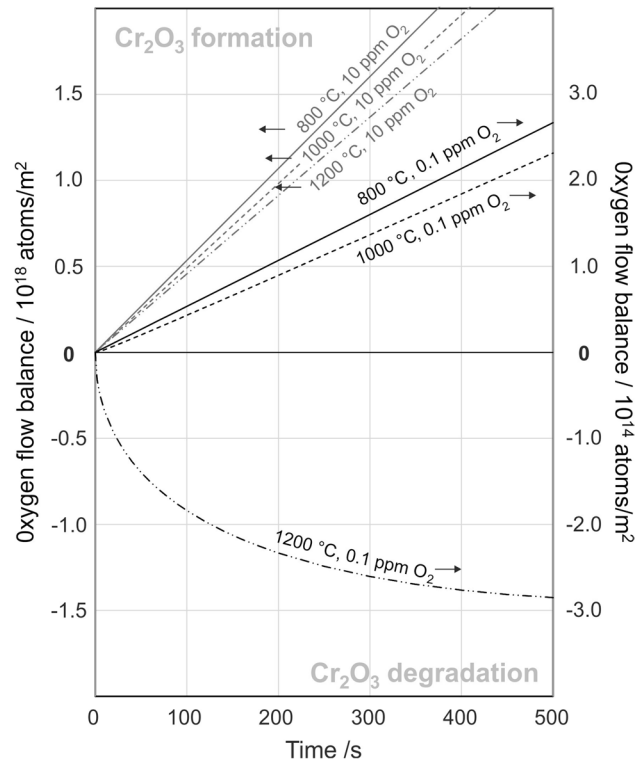
extremely low oxygen residue), while ferritic Cr steels need even higher temperatures (approx. + 100 °C) and lower oxygen (resp. water) residues in the process atmosphere. The latter can be also explained by the physical model. The temperature dependent solubility of oxygen is smaller in the bcc lattice of a ferritic steel (α-Fe) than in the austenitic fcc lattice (γ-Fe) at the same temperature. In [6] numerical equations for the maximum solubility of oxygen in bcc- and fcc-Fe (in equilibrium with FeO) are given as a function of temperature, cf. Eqs. (24) and (25).

$$\log(w_{O-\max}) = -4700/T + 0.3 \quad (\gamma - \text{Fe}) \qquad (24)$$

$$\log(w_{O-\max}) = -7140/T + 2.05 \quad (\alpha - \text{Fe}) \qquad (25)$$

At 1000 °C, for example, a maximum O-concentration in γ-Fe of 4.1×10^{-4} wt% is obtained, while in α-Fe the oxygen solubility is computed to be 30% lower (2.7×10^{-4} wt%) at the same temperature. The lower solubility of oxygen in the ferritic steel leads to a stronger increase of the oxygen activity compared to the austenitic steel and oxygen absorption reaches its limit faster in the ferritic steel. Therefore, oxygen transport into steel by diffusion is reduced in a ferritic steel, which in turn must be compensated by higher process temperatures. Arithmetically, the solubility of oxygen in α-Fe

is at 1050 °C the same as in γ-Fe at 1000 °C according to Eqs. (24) and (25).

Furthermore it is well-known, that when brazing unalloyed steels, the demands on process atmosphere quality are distinctly lower due to the absence of chromium (and chromium oxide in the oxide layer) and a good spreading of AgCu braze can already be achieved at 900 °C [11]. In contrast, aluminium containing ferritic Cr-steels are said to be non-brazeable, since the aluminium oxide in the oxide layer is thermodynamically extremely stable [12]. Therefore, it does not decompose in the form described by the physical model (see Eq. 1 and following) at typical brazing temperatures, even if the oxygen partial pressure in the furnace atmosphere is extremely low.

Despite of the empirical knowledge on brazeability, experimental analyses and a detailed understanding of the mechanism of metal surface deoxidation and wetting on the atomic scale are still missing, although this is essential for the advancement of brazing technology and other industrial processes, where metallurgical interactions between contacting metallic surfaces play a key role. In this context, welding, thermal coating, sintering or the new, rapidly growing technology of additive manufacturing are prominent examples.

## 3 Surface Deoxidation Under Hydrogen

Reducing hydrogen as the process gas is widely used in furnace brazing to promote oxide layer decomposition [13]. In principle, the reduction of a metal oxide by hydrogen is possible according to

$$2yH_2(g) + M_xO_{2y}(s) \rightarrow 2yH_2O(g) + xM(s). \tag{26}$$
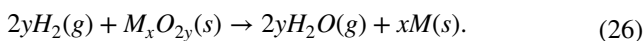
provided that the necessary thermodynamic conditions for this reaction are fulfilled. The thermodynamic stability of the oxide is determined by its free enthalpy of formation. According to Eq. (5), the free enthalpy of formation is connected with the oxygen activity of the oxide. For modelling the oxide layer degradation, the oxygen activity has to be related to its gaseous molecular state, and thus, the factor 2 in the exponential term of Eq. (5) must be cancelled only to use this relation for the evaluation of the activity of molecular oxygen.

In Fig. 5, the gaseous oxygen activities are plotted as a function of temperature for a variety of metal oxides representing the oxide layers of typical metallic structural materials. The low oxygen activities of the different metal oxides indicate, that a thermal decomposition of most of these oxides do not take place under the conditions of a brazing process in a vacuum furnace. Only the copper oxide (Cu_2O) and the nickel oxide (NiO) could decompose, whereupon in the case of NiO a temperature of at least 1100 °C and a

good vacuum level (10^{-5} mbar) are necessary. The curves (continuous lines) show two important properties: first with decreasing noble character of the metal, the corresponding oxide becomes increasingly more stable. This is reflected in the decreasing oxygen activities in the order Cu, Ni, Fe, Zn, Cr, Mn, Si, Ti and Al, which vary over many orders of magnitude. In addition, the oxygen activity in each case increases with temperature, and thus, the stability of each oxide decreases at elevated temperatures. Analogous to the metal oxides the oxygen activity in the presence of water, i.e.:

$$2H_2(g) + O_2(g) \leftrightarrow 2H_2O(g), \tag{27}$$
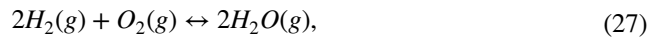
can be evaluated in the same way. The equilibrium constant for Eq. (27) is:

$$K_a(T) = \frac{[a_{H_2O}]^2}{[a_{H_2}]^2[a_{O_2}]}. \tag{28}$$

In contrast to the metal/metal oxide systems all reactants form a gaseous mixture now. Since the activity of a gas at moderate pressure is equal to its partial pressure divided by the standard pressure (101,325 Pa), inserting Eq. (28) in Eq. (4) gives the equilibrium oxygen activity in a hydrogen atmosphere as a function of temperature and water content:

$$a_{O_2} = \left(\frac{p_{H_2O}}{p_{H_2}}\right)^2 \exp\left(\frac{\Delta_f G^o_{H_2O}(T)}{RT}\right). \tag{29}$$

In Fig. 5 the dashed lines show the resulting oxygen activities for different water contents. Here the curve denoted with "H_2/H_2O" represents the special case $p_{H_2O} = p_{H_2}$ where a direct comparison of the oxygen affinity of hydrogen to those of the various metals is possible.
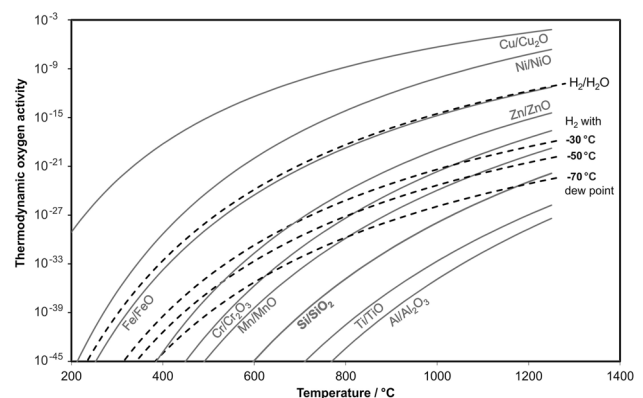

Fig. 5 Oxygen activities of metal oxides (continuous lines) and those in hydrogen with different water content (dashed lines) as calculated from their free enthalpies of formation; thermodynamic data are from Ref. [3]

In fact, this affinity is close to the one of metallic iron, cf. Fig. 5. Much lower oxygen activities and therefore higher oxygen affinities can be reached by substantially lowering the water content, which is usually defined by the dew point of the hydrogen. Typical dew points in (continuous) furnace processes are between − 30 °C (= 300 ppm water vapour residue) and − 50 °C (40 ppm). Currently, the technical limit for the hydrogen dew point in such processes is governed by the purity of the process gas used and is about − 70 °C (2 ppm). The corresponding curves for this dew points are also plotted in Fig. 5. The hydrogen curves have a shape similar to those of the metals, but their slope at higher temperatures tends to be significantly lower.

The interpretation of the data with respect to the chemical reducibility of the metal oxides by hydrogen is straightforward. For a given "hydrogen curve" at a fixed temperature all metal oxides can be reduced, if their oxygen activities are higher at this temperature, while the other metal oxides remain unchanged. Furthermore, metals with lower oxygen activities of their oxide than that of the hydrogen atmosphere used are even oxidised by the given water residue (dew point) of the gas.

In the case of a chromium oxide layer on a metal surface, a temperature of at least 1050 °C is necessary for its reduction, when the process is performed under hydrogen with a dew point of − 30 °C. At lower temperature, further growth of the chromium oxide takes place, since the water residue acts as an oxidising agent with considerable oxide growth rates due to its high concentration of 300 ppm. By contrast, the point of inflection between growth and reduction of chromium oxides is already at about 800 °C in hydrogen with a dew point of − 50 °C (40 ppm water residue). Obviously, high brazing temperatures (up to 1200 °C) and low dew points are favourable for brazing high chromium steels under hydrogen. This is even more so, as these steel qualities often contain low concentrations of still more oxygen affine elements like Mn, Mo, Si or Ti. Furthermore, it becomes clear from the thermodynamic analysis that generally it is not possible to reduce oxide layers on light metal alloys based on titan, aluminium or magnesium, using a hydrogen atmosphere.

Although the use of hydrogen for industrial furnace processes is state-of-the-art, there are significant disadvantages related to this technology. Storage, distribution and handling of hydrogen requires high safety precautions. Especially in continuous working conveyor belt furnaces with their openings a controlled flare of the exiting process gas must be insured, in order to avoid explosive air-hydrogen mixtures outside the furnace. In fact, an ordinary conveyor belt furnace for brazing stainless steel components has an annual hydrogen consumption of 150,000 cubic meters, which is not used energetically in any way. This amount corresponds to a calorific value of approx. 50,000 l of fuel oil.

4 SiH$_4$-Doped Inert Gases for Oxygen-Free Processes

An attractive alternative to hydrogen is the use of monosilane-doped inert process gases (argon or nitrogen) in furnace brazing [14]. Monosilane (SiH$_4$) is a metastable gas, which has almost the same oxygen affinity than (solid) silicon (Si). Figure 6 reveals the high potential of this gas. Especially at lower temperature silicon has a very much lower oxygen activity than hydrogen with dew point of − 70 °C. Furthermore, monosilane is highly reactive to oxygen and unrestricted gaseous reactions with oxygen and water take place already at room temperature [15]. Consequently, mixing monosilane to an inert gas leads to a quantitative elimination of all oxygen and water residues according to the reactions

$$SiH_4(g) + 2O_2(g) \rightarrow SiO_2(s) + 2H_2O(g) \tag{30}$$

$$SiH_4(g) + 2H_2O(g) \rightarrow SiO_2(s) + 4H_2(g). \tag{31}$$
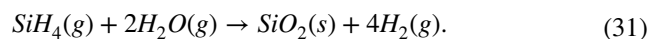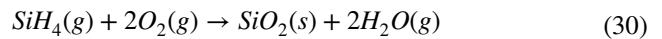
In detail these gas reactions are radical chain reactions, where a large number of intermediate products are involved [16]. Therefore, a thermodynamic analysis of a monosilane-doped inert gas with respect to the resulting oxygen activities was done by numerical methods. Using the commercial software FACTSAGE© (GTT Technologies, Herzogenrath, Germany) the thermodynamic equilibrium conditions in Argon with defined initial oxygen residues where calculated at different temperatures, after adding increasing amounts of monosilane to the gas. For this a data base was employed, where the temperature dependent free enthalpies of formation of all hypothetical reaction products formed from Si,
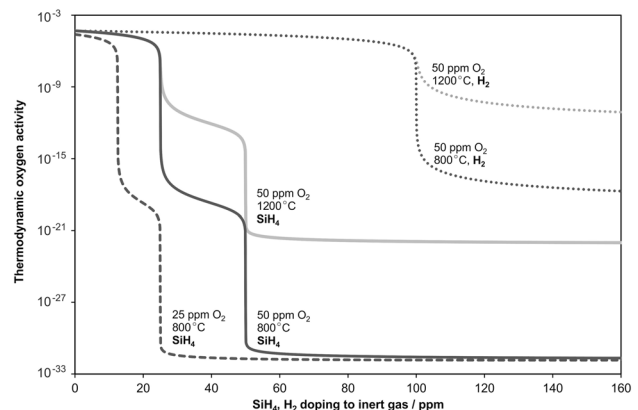

Fig. 6 Calculated decrease of oxygen activity with increasing admixture of SiH$_4$ or H$_2$ to an inert gas with defined initial O$_2$ residues (25 ppm, 50 ppm) at 800 °C and 1200 °C

O, and/or H are filed as a function of temperature. In the calculation the amount of each product in the gas mixture is adjusted such that the sum of the free enthalpies of formation is minimal, which defines the condition for thermodynamic equilibrium in a multi-component system.

The resulting oxygen activities for different system conditions (gas temperature: 25 °C, 800 °C, 1200 °C; initial oxygen residue: 25 ppm, 50 ppm) are plotted in Fig. 6. In addition, the admixture of hydrogen instead of monosilane for eliminating the oxygen (see Eq. 27) is included for comparison. Looking at the results for doping with monosilane, the two step reaction of SiH_4 with O_2 according to Eqs. (30) and (31) are clearly visible. When the admixed SiH_4 concentration is half of the initial O_2 concentration there is a first abrupt decrease of oxygen activity over about 10 orders of magnitude indicating the quantitative reduction of O_2 to SiO_2 and H_2O (Eq. 30). A second stepwise drop of the curves take place at stoichiometrical equality (initial O_2 concentration equal to admixed SiH_4 concentration), where the formed H_2O is eliminated quantitatively according to Eq. (31), resulting in extremely low oxygen activities ($< 10^{-32}$ at 800 °C and $< 10^{-21}$ at 1200 °C) of the doped inert gas.

In view of Fig. 5, doping conventional inert process gases (e.g. Ar or N_2 with O_2 residues of 10–50 ppm) with only little amounts of monosilane (< 100 ppm) yields oxygen activities, which are much lower than the values in pure hydrogen especially at moderate process temperatures. Specifically, a doping with H_2 yields much higher oxygen activities after quantitative reduction of all O_2 to H_2O according to Eq. (27), when the H_2 admixture exceed twice the initial O_2 concentration. According to Fig. 6 the values reached are of the order of 10^{-11} and 10^{-18} at 800 °C and 1200 °C, respectively. Of course, these are very close to the corresponding values of the H_2/H_2O curve in Fig. 5, since the thermodynamic conditions considered in both cases are quite similar.

5 Application of SiH₄-Doped Process Gases for Brazing in Controlled Atmosphere

Process gas conditioning with monosilane was experimentally tested in a conveyor belt furnace, which was equipped for brazing processes up to 1200 °C under nitrogen, argon and/or hydrogen. The system had been upgraded with an additional gas flow controller, which allowed the precise addition of monosilane (pre-diluted in argon) to the process gas used, in order to realize monosilane concentrations in the gas between 1 and 100 ppm. When operating the furnace, a permanent control of the oxygen residues was realized by continuous sampling process gas from the heating zone and analysing it with a calibrated lambda oxygen sensor, allowing the reproducible detection of thermodynamic oxygen activities down to 10^{-22}.

In Fig. 7 the evolution of the oxygen activity in the furnace with a stepwise increase of monosilane admixture (in nitrogen as process gas) over a period of about 5 h is plotted. Between every step of increase, the system was allowed to reach stationary conditions, i.e. the measuring signal did not change significantly anymore (typically after 15–30 min). The gas temperature in the furnace was 600 °C, which was identical with the working temperature of the oxygen sensor. As predicted by the thermodynamic modelling, an abrupt decrease of oxygen activity was observed, when half of the initial oxygen residue (in this case 13.5 ppm O_2) was added to the nitrogen, reaching an oxygen activity of about 10^{-21}. A further increase of monosilane led to a further decrease of measured oxygen activity. However, the second drop of the curve—as predicted at equal stoichiometry of added SiH_4 and initial O_2 content—was not measureable. This is due to the principal physical limitations of measuring such low oxygen activities in a gas.

Brazing experiments with numerous parent materials and braze metals—covering the spectrum of industrial relevant furnace brazing applications—where performed using monosilane doped process gases Two examples are illustrated in the following. In the first case, Fig. 8, a typical assembly made from stainless steel, which is usually brazed with Cu braze in a conveyor belt furnace under pure hydrogen, was successfully processed in the furnace under SiH_4-doped nitrogen.

The second example, Fig. 9, represents an assembly made of titanium and WC/Co-hard metal, a material combination, which is usually brazed with an AgCu braze alloy in a high vacuum furnace. Due to the extremely high oxygen affinity especially of the titanium, a vacuum level of 10^{-5} mbar is essential for a successful brazing. Using SiH_4-doped argon such a brazing operation is now possible in a continuous working belt furnace. Note that even monosilane is not able to reduce titanium oxide. However, it effectively prevents
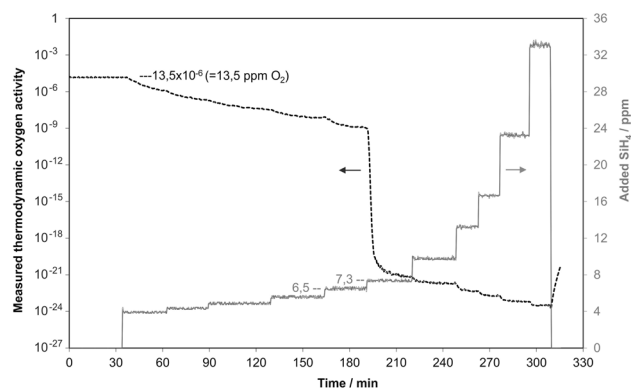
Fig. 7 Evolution of thermodynamic oxygen activity in a conveyor belt furnace under nitrogen with increasing admixture of monosilane; dashed line: measured thermodynamic oxygen activity (left y-axis), continuous line: monosilane concentration (right y-axis)

Fig. 8 Stainless steel components joint with copper braze at 1100 °C in a conveyor belt furnace under SiH_4-doped nitrogen. Right: optical microscopy image of a cross section from a joint
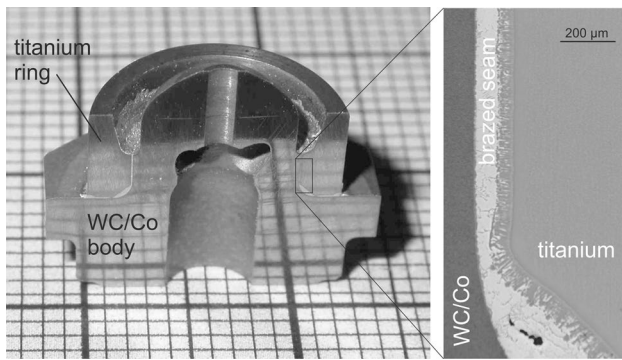

Fig. 9 Metallographically prepared titanium/hard metal (WC/Co) component, joint with $Ag_{72}Cu$ brazing alloy at 820 °C in a conveyor belt furnace under SiH_4-doped argon; detail to the right: optical microscopy image of a cross section from the joint

titanium from further oxidation upon heating. Thus, the native titanium oxide layer can be decomposed by oxygen diffusion into the bulk material, since titanium has a high solubility for oxygen at elevated temperature. The $Ag_{72}Cu_{28}$ braze used features a melting point of 780 °C and can wet the titanium. Next, titanium is solved in the liquid braze forming "in situ" an active braze, which in turn wets the hard metal excellently.

A variety of other material combinations, which can be brazed without flux under SiH_4-doped nitrogen especially at moderate temperatures (< 850 °C) are described in [17].

The use of monosilane-doped inert gases instead of pure hydrogen or high vacuum offers substantial economical and resource-saving potentials for furnace brazing and similar heat treatment processes. Nevertheless, operational safety requirements of this technology have to be considered as well. With the elimination of oxygen and water by monosilane the formation of solid SiO_2 results (Eqs. 30 and 31). At stoichiometric admixture of SiH_4 the amount of formed SiO_2 in gram per hour is given by
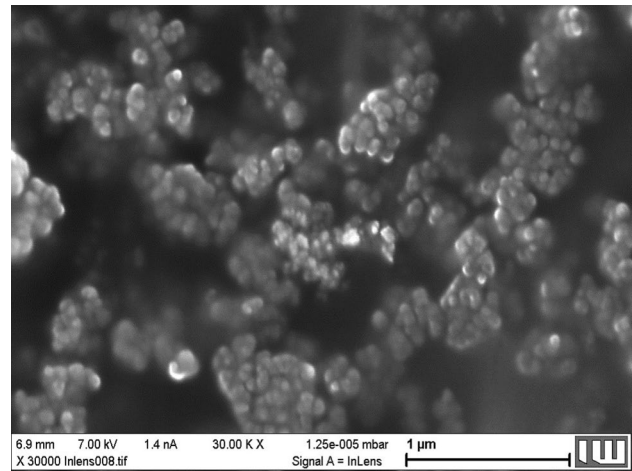

Fig. 10 SEM image of amorphous SiO_2 dust sampled at the input opening of the conveyor belt furnace after operating the furnace under SiH_4-doped nitrogen

$$\frac{\dot{m}_{SiO_2}}{g \cdot l^{-1}} = 2.5 \cdot 10^{-3} \frac{\dot{V}_{gas}}{m^3 \cdot h^{-1}} \left(\frac{X_{O_2}}{ppm} + \frac{1}{2} \frac{X_{H_2O}}{ppm} \right), \tag{32}$$

as a function of the consumed inert gas volume per hour and its oxygen and water residues that are to be eliminated by monosilane. The conveyor belt furnace described above consumes 10 m^3/h inert gas. Assuming the measured initial oxygen residue of 13.5 ppm (and no initial water content) roughly 0.4 g SiO_2 per hour are generated, which is emitted with the exiting process gas. It is important to note, that the generated SiO_2 is pyrophoric, forming dust from agglomerated amorphous silicon oxide spheres of approx. 50 nm diameter, cf. Fig. 10. In contrast to crystalline silica, the amorphous species is quite uncritical and is, due to its notable solubility in water, metabolizable to a certain extent, when inhaled [18]. Still, the emission must meet general boundary values for respirable dust. The threshold limit value in ambient air for such fine dust (class PM2.5) is 1.25 mg/m^3 [19]. Thus, the furnace used was equipped with an exhaust system with 1000 m^3/h capacity, which ensures an effective cleaning of the air around the furnace openings and a sufficient dilution of the sucked process gas with air before releasing it to the environment.

6 Discussion

For flux-free brazing, the degradation rate of the oxide layer is key to success of the joining process. In absence of a reducing agent, this rate is governed by the thermally activated diffusion of oxygen and is restricted at the same time by the thermodynamic stability of the oxide species

to be removed. An additional disruptive factor is the re-oxidation of the metal surface during heat treatment due to oxygen residues present in the inert gas. The rate of re-oxidation, estimated by a gas-kinetic approach, is proportional to the square of the residual oxygen concentration in the gas. Balancing the arising oxygen mass flows as a function of the process parameters (temperature, dwell-time, oxygen residue) for the materials (metal/oxide systems) to be processed, appropriate process parameters and limiting factors for oxide layer degradation can be found. For instance, to avoid a significant oxidation of chromium containing steel, oxygen residues < 1 ppm should be aimed at, when brazing under inert gas.

Furthermore, the thermodynamic conditions for oxide layer decomposition in reducing hydrogen atmosphere and the role of its water content (dew point) has been analyzed. It is demonstrated that especially at moderate temperatures the reducing effect of hydrogen is quite limited even at low dew points. In addition, at low temperatures the reactivity of hydrogen is generally low, which is mirrored by its high autoignition temperatures (> 500 °C) under different reaction conditions [20]. Therefore, hydrogen is generally inapplicable as a reducing agent for moderate temperatures, even at low dew point. In fact, dew points lower than − 50 °C (equal to 40 ppm H_2O residue) can hardly be reached in conventional hydrogen furnaces. Exceeding of the water content above the thermodynamic limit for an oxide layer reduction, leads in turn to a drastic oxidation of the metal considered, since not only oxygen but also water vapor is a good oxidant for most structural metals especially at elevated temperatures. In fact, brazing under reducing hydrogen with a poor dew point is inevitable worse than using inert gas, e.g. nitrogen or argon, with low oxygen residue.

With respect to safety and in terms of a sustainable production, the use of hydrogen as the process gas has disadvantages: The transport, storage and handling of hydrogen calls for special safety measures, which makes production using this gas costly. Furthermore, hydrogen is produced mostly via steam reforming from fossil energy sources (natural gas, mineral oil, coal). Therefore, its consumption, especially in such an ineffective way like in the furnace processes described, considerably contributes to the carbon dioxide emission in industrial production.

The use of monosilane-doped inert gases is a very attractive alternative to generate almost absolutely oxygen-free process environments in a quite simple, cost-efficient and environmental friendly way. Due to its extremely high oxygen affinity, already the admixture of very small amounts of SiH_4 (< 100 ppm) drastically lowers the oxygen activity in conventional inert gases used for furnace processes (Ar, N_2). This results in process conditions, which are much better than those obtainable under very dry hydrogen conditions. Because of the low SiH_4

concentrations needed with this approach, the monosilane can be applied as pre-diluted gas mixture (e.g. 1 vol.% SiH_4 in Ar) for doping the process gas. This makes it easy to handle the gas, since no explosion protection arrangements are required.

So far SiH_4-doped inert gases have been successfully tested in furnace brazing and heat treatment processes with process temperatures > 500 °C. In fact, because of the thermally unrestricted reactivity of SiH_4 to oxygen, the quantitative elimination of any oxygen residue in the inert gas takes place already at room temperature. This makes SiH_4-doped inert gases also attractive for processes, where oxygen-free process atmospheres at ambient temperatures are requested and a total encapsulation of the process from the environment is costly or generally not possible. For instance, this may be applied to additive manufacturing processes, where locally an oxygen free environment is needed for processing oxidation sensitive metallic powders by means of laser melting [21, 22]. Finally, any emission of process gas into the environment is not critical, as the SiH_4 reacts to form harmless amorphous SiO_2.

7 Conclusions

- Neither heat treatment in vacuum furnaces nor under conventional protective gases ensure process conditions, which are really oxygen-free. Thus, deoxidation of materials surfaces is key step for wetting with braze metal.
- Deoxidation at flux-free brazing of steels under vacuum or inert atmosphere can happen based upon thermal activation of oxygen diffusion from the oxide layer into the molten braze metal and the parent metal.
- The decomposition rate of oxide layer depends on the chemical composition of the steel and the oxide layer, the braze metal and the process temperature, and is governed by the thermodynamic stability of the oxide to be decomposed.
- Significant decomposition of iron oxide layers on austenitic steels starts at 900 °C, while for a decomposition of chromium oxide temperatures above 1200 °C are necessary.
- Re-oxidation of the stainless steel surfaces during brazing under inert process gases is a key problem when using only technical gas qualities, as level of oxygen and water residue should be kept below 1 ppm to avoid re-oxidation.
- The reduction of oxide layers with hydrogen is limited by the thermodynamic stability of the oxides, the reaction temperature and the level of water residue (dew point) in the process atmosphere.
- Doping of conventional inert gases like N_2 or Ar with SiH_4 (monosilane) leads to a quantitative elimination of

oxygen and water residues, and constitute process conditions, which are even better than under very dry hydrogen (dew point $< -70\ °C$).

- The necessary concentration of SiH_4 in the gas depends on the oxygen residue to be eliminated. Concentrations of 10 ppm to 100 ppm SiH_4 are sufficient for technical inert gases. The low SiH_4 concentrations needed provide for an easy handling of SiH_4-doped inert gases as the gas mixture is not toxic nor explosive.
- SiH_4-doped inert gas is a cost-efficient, safe and environmental friendly alternative to hydrogen as process gas.

Compliance with Ethical Standards

Conflict of interest On behalf of all authors, the corresponding author states that there is no conflict of interest.

References

1. Roberts, P. (2013). *Furnace brazing. Industrial brazing practice* (2nd ed., pp. 187–241). Boca Raton: CRC Press.
2. Kozlova, O., Voytovych, R., Devismes, M.-F., & Eustathopoulos, N. (2008). Wetting and brazing of stainless steels by copper–silver eutectic. *Materials Science and Engineering: A, 495,* 96–101. https://doi.org/10.1016/j.msea.2007.10.101.
3. Bach, F.-W., Möhwald, K., & Holländer, U. (2010). Physicochemical aspects of surface activation during fluxless brazing in shielding-gas furnaces. *Key Engineering Materials, 438,* 73–80.
4. Paul, A. (1982). *Oxidation–reduction equilibrium in glass. Chemistry of glasses* (p. 148). London: Chapman and Hall Ltd.
5. Osterwald, J., Reimann, G., & Stichel, W. (1969). Über die Sauerstoffaktivität in flüssigem Kupfer. *Zeitschrift für Physikalische Chemie, 66,* 1–7.
6. Dieckmann, R. (1983). Punktfehlordnung, nichtstöchiometrie und transporteigenschaften von oxiden der übergangsmetalle kobalt, eisen und nickel (Professorial Dissertation, Faculty of Chemistry, Leibniz Universität Hannover, 1983).
7. Oberg, K. E., Friedman, L. M., Boorstein, W. M., & Rapp, R. A. (1973). The diffusivity and solubility of oxygen in liquid copper and liquid silver from electrochemical measurements. *Metallurgical and Materials Transactions B, 4*(1), 61–67.
8. Takada, T., Yamamoto, S., Kikuchi, S., & Adachi, M. (1986). Determination of diffusion coefficient of oxygen in gamma-iron from measurements of internal oxidation in Fe–Al alloys. *Metallurgical Transactions A, 17,* 221–229.
9. Kerber, S. J., & Tverberg, J. (2000). Stainless steel surface analysis. *Advanced Materials and Processes, 158*(5), 33–36.
10. Lide, D. R. (2008). *Physical constants of inorganic compounds. Handbook of chemistry and physics* (89th ed.). Boca Raton: CRC Press.
11. Müller, W., & Müller, J.-U. (1995). *Löttechnik: Leitfaden für die Praxis*. Düsseldorf: Deutscher Verlag für Schweißtechnik DVS Verlag GmbH.
12. Strauß, C., Gustus, R., Maus-Friedrichs, W., Schöler, S., Holländer, U., & Möhwald, K. (2019). Influence of atmosphere during vacuum heat treatment of stainless steels AISI 304 and 446. *Journal of Materials Processing Technology.* https://doi.org/10.1016/j.jmatprotec.2018.08.038.
13. Stratton, P. F. (2004). *Hydrogen for furnace brazing stainless steel: optimizing sourcing and application. DVS-Berichte* (Vol. 231, pp. 181–184). Düsseldorf: DVS-Media.
14. Bach, F.-W., Möhwald, K., Holländer, U., & Roxlau, C. (2007). *SCIB-Self-cleaning inert-gas brazing-Ein neues Verfahren zum flussmittelfreien Hartlöten korrosionsbeständiger Konstruktionswerkstoffe. DVS-Berichte* (Vol. 243, pp. 235–241). Düsseldorf: DVS-Verlag.
15. Tamanini, F., Chaffee, J. L., & Jambor, R. L. (2004). Reactivity and ignition characteristics of silane/air mixtures. *Process Safety Progress, 7*(4), 243–258. https://doi.org/10.1002/prs.680170405.
16. Quandt, R. W., & Hershberger, J. F. (1993). Kinetics of the $SiH_3 + O_2$ and $SiH_3 + NO_2$ reactions. *Chemical Physics Letters, 206,* 355–360.
17. Holländer, U., Weber, F., Möhwald, K., & Maier, H. J. (2016). Development of processes for flux-free gas-shielded brazing between 650 °C and 850 °C utilising silane-doped process gases. *Welding and Cutting, 15*(4), 248–258.
18. Johnston, C. J., Driscoll, K. E., Finkelstein, J. N., Baggs, R., O´Reilly, M. A., Carter, J., et al. (2000). Pulmonary chemokine and mutagenic responses in rats after subchronic inhalation of amorphous and crystalline silica. *Toxicological Sciences, 56,* 405–413.
19. Bundesamt Für Arbeitsschutz und Arbeits-Medizin-Ausschuss Für Gefahrenstoffe, 2018. Technische regeln für gefahrstoffe (TRGS) 900: „Arbeitsplatzgrenzwerte". Ausgabe: Januar 2006, zuletzt geändert und ergänzt: 07.8.2018. Retrieved February 04, 2019, from https://www.baua.de/DE/Angebote/Rechtstexte-und-Technische-Regeln/Regelwerk/TRGS/TRGS-900.html.
20. Conti, R. S., & Hertzberg, M. (1988). Thermal autoignition temperatures for hydrogen-air and methane-air mixtures. *Journal of Fire Sciences, 6*(5), 348–355.
21. Khademzadeh, S., Parvin, N., & Bariani, P. F. (2015). Production of NiTi alloy by direct metal deposition of mechanically alloyed powder mixtures. *International Journal of Precision Engineering and Manufacturing, 16,* 2333. https://doi.org/10.1007/s12541-015-0300-1.
22. Chua, Z. Y., Ahn, I. H., & Moon, S. K. (2017). Process monitoring and inspection systems in metal additive manufacturing: Status and applications. *International Journal of Precision Engineering and Manufacturing-Green Technology, 4,* 235. https://doi.org/10.1007/s40684-017-0029-7.

Ulrich Holländer studied chemistry and received his Doctoral Degree in Natural Sciences from the Technical University of Dortmund in 1997. Since 2002, he has been scientific assistant at the Leibniz University of Hanover conducting the research group "Brazing and Thermal Process Technology" at the Institute of Materials Science. His current research interests include the development of materials and processes for flux-free brazing and thermal coating.

Daniel Wulff studied physics at the University of Wuppertal and continued his academic education at the Leibniz University of Hanover receiving the Doctoral Degree in Mechanical Engineering in 2018. Since 2018, he has been employee at the Institute for Damage Prevention and Damage Research in Kiel. His current engagement is on the investigation of damages on tap water installations caused by material defects and faulty joints.

André Langohr received his diploma in Chemistry from the Technical University of Dortmund in 1992. Since 2005, he is scientific assistant at the Institute of Materials Science, Leibniz University of Hanover. His research interests include the computational thermodynamic modelling of materials and chemical reactions concerning brazing processes under vacuum and process gases.

Kai Möhwald received his Doctoral Degree in Mechanical Engineering from the Technical University of Dortmund in 1996. He continued his academic career at Leibniz University of Hanover and habilitates in 2009 receiving the Venia Legendi for Materials Engineering. Since 2015, he has been Associate Professor at the Leibniz University of Hanover. He is divisional head of the department "Surface and Joining Technology" at the Institute of Materials Science. His research interests include Brazing Technology, Thermal Coating Technology and Hybrid Technologies.

Hans Jürgen Maier received his Doctoral Degree in Materials Science from the Friedrich-Alexander University (FAU) of Erlangen-Nürnberg in 1990 and continued his engagement at FAU as Post-Doc until 1993. From 1993 to 1999, he was Senior Research Engineer at the University of Siegen. From 1999 to 2012, Hans Jürgen Maier was Chair Professor for Materials Science at the University of Paderborn. Since 2012, he has been Chair Professor and Director of the Institute for Materials Science at the Leibniz University of Hanover. His research interests include Microstructure-Property-Relationship in Advanced Metallic Materials, Thermomechanical Fatigue Behaviour, Material Modelling, Heat Treatment and Phase Transformation.